Supporting Information for

Studies of the hydrophobic interaction between a pyrene - containing dye and a tetra-aza macrocyclic gadolinium complex

Enza Di Gregorio,[a] Mariangela Boccalon,[b] Chiara Furlan,[c] Eliana Gianolio,[a,c] Attila Bényei,[d] Silvio Aime,[c] Zsolt Baranyai,[b,*] Giuseppe Ferrauto[a,*]

[a] Molecular Imaging Center, Department of Molecular Biotechnologies and Health Sciences, University of Torino, Via Nizza 52, 10126, Torino (TO), Italy

[b] Bracco Imaging spa, Bracco Research Centre, Via Ribes 5, 10010 Colleretto Giacosa (TO), Italy

[c] IRCCS SDN Research Institute Diagnostics and Nuclear SynLab, Via Emanuele Gianturco, 113, 80143 Napoli (NA), Italy

[d] Department of Physical Chemistry, University of Debrecen, H-4010, Debrecen, Egyetem tér 1., Hungary

Corresponding Authors:

Zsolt Baranyai

Bracco Imaging – CRB/Trieste,
Area Science Park. Ed. Q, SS 14, km 163.5, I-34149, Basovizza Trieste, Italy.
tel. +39 040375-7842
fax +39 0403757831
email: zsolt.baranyai@bracco.com

Giuseppe Ferrauto

Molecular Imaging Center, Department of Molecular Biotechnologies and Health Sciences, University of Torino, Via Nizza 52, 10126, Torino (TO), Italy
tel. +39 0116708459
fax +39 0116706487
email: giuseppe.ferrauto@unito.it

Table of Content:

I. Spectrophotometric and spectrofluorometric studies of the interaction between Gd(HP-DO3A) and HPTS

I.1 Spectrophotometric studies

The protonation constant of HPTS (T), defined by Eq. (S1), have been determined by spectrophotometry.

$$T + H^+ \rightleftharpoons HT \qquad \text{(S1)}$$

$$K^H = \frac{[HT]}{[T][H^+]}$$

Protonation/deprotonation of the phenyl -OH group has been studied by spectrophotometry on the absorption band of the HPTS, following the absorbance values at 300, 375, 405 and 455 nm. The Vis-spectra and the absorbance values at 300, 375, 405 and 455 nm of the HPTS are shown in Figure S1. The absorbance of HPTS is a combination of the absorption of each protonated species and expressed by Eq. (S2).[1]

$$A = \sum [H_i T] \varepsilon_{H_i T} l \qquad \text{(S2)}$$

where, A is the absorbance at a given wavelength, $[H_iT]$, ε_{HiT} and l are the concentration and the molar absorptivity of the species and the path length of the cell, respectively. The observed absorbance values (A) have been fitted to the Eq. (S2) (the concentration of the different protonated species has been expressed by the protonation constants K^H, Eq. (S1)). The fittings of the experimental data points are shown in Figure S1. The protonation constant of the HPTS was found to be logK^H=7.10 (8) at 25°C in 0.15 M NaCl solution (standard deviations are shown in parentheses).

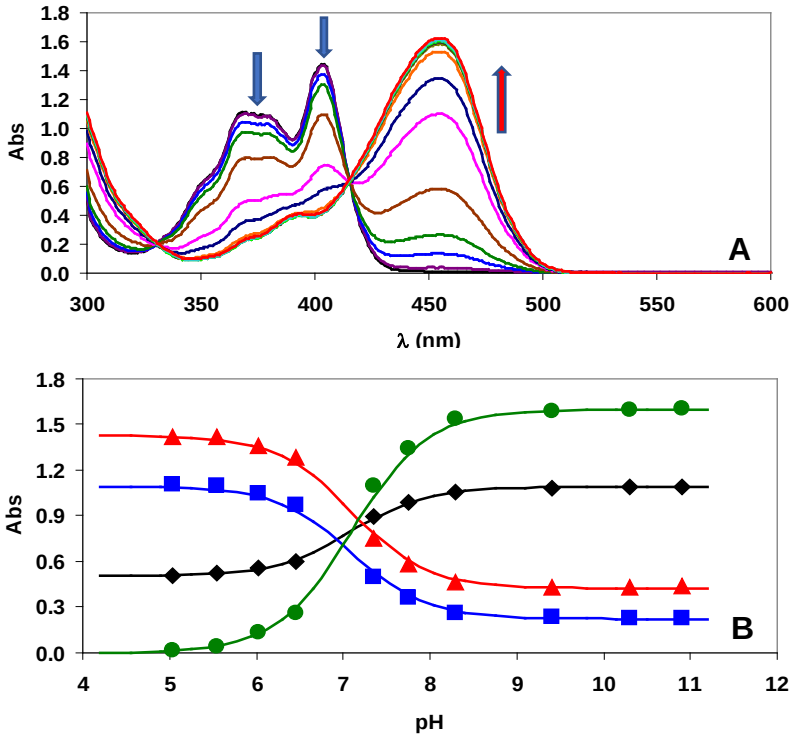

Figure S1. Absorption spectra (**A)** and absorbance values (**B**) of HPTS as a function of pH at 300 (◆), 370 (■), 405 (▲) and 455 nm (●). The solid lines and the symbols represent the experimental and the calculated absorbance values, respectively. ([HPTS]=50 μM, 0.15 M NaCl, 25°C)

I.2 Spectrofluorometric studies

To characterize the interaction between HPTS and Gd(HP-DO3A), emission spectra of the HPTS – Gd(HP-DO3A) systems have been recorded with λ_{exc} = 405 and 455 nm and a slitwidth of 3 nm in the wavelength range 460 – 700 nm ([HPTS]=100 nM, [Gd(HP-DO3A)]=0 – 2.0 mM, 0.15 M NaCl). Emission spectra of HPTS – Gd(HP-DO3A) systems are shown in Figures S2 – S7.

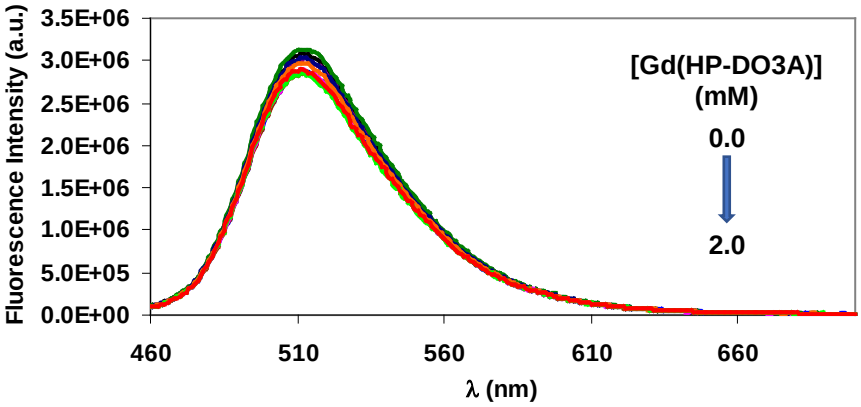

Figure S2. Emission spectra of HPTS in the presence and absence of Gd(HP-DO3A) ([HPTS]=100 nM, [Gd(HP-DO3A)]=0 - 2 mM, pH=6.5, λ_{exc}=405 nm, 0.15 M NaCl, 25°C)

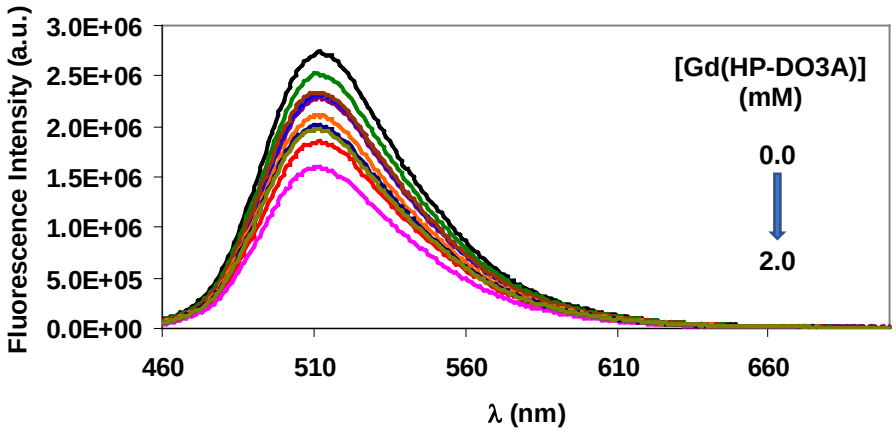

Figure S3. Emission spectra of HPTS in the presence and absence of Gd(HP-DO3A) ([HPTS]=100 nM, [Gd(HP-DO3A)]=0 - 2 mM, pH=7.0, λ_{exc}=405 nm, 0.15 M NaCl, 25°C)

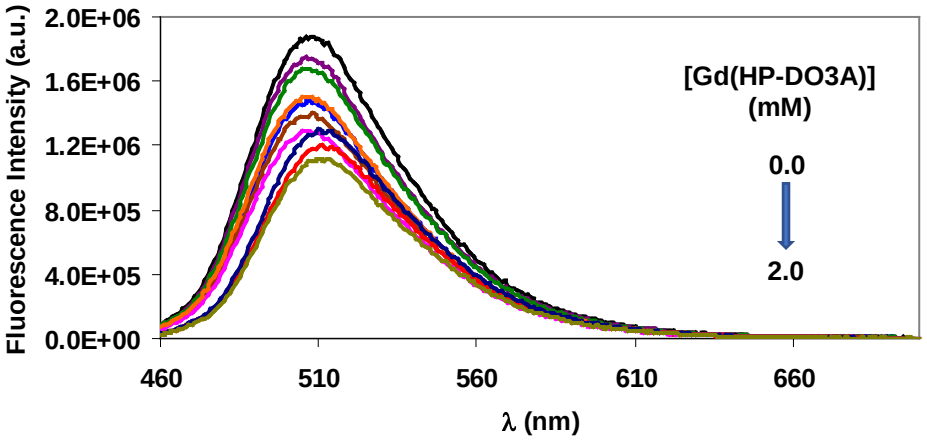

Figure S4. Emission spectra of HPTS in the presence and absence of Gd(HP-DO3A) ([HPTS]=100 nM, [Gd(HP-DO3A)]=0 - 2 mM, pH=8.0, λ_{exc}=405 nm, 0.15 M NaCl, 25°C)

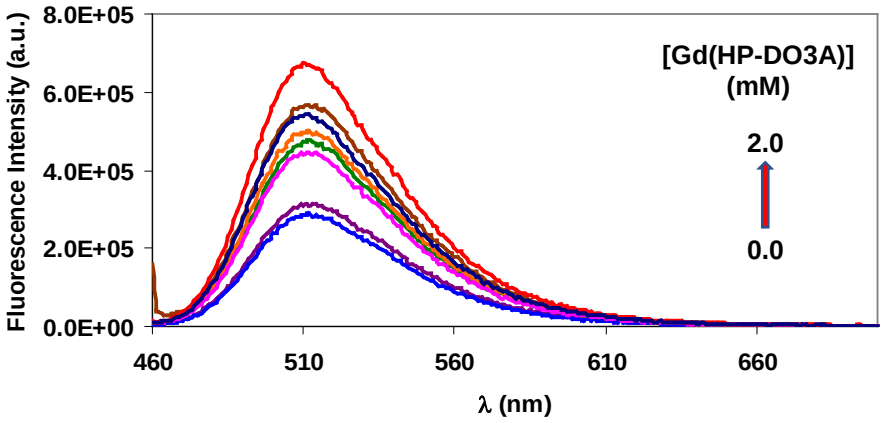

Figure S5. Emission spectra of HPTS in the presence and absence of Gd(HP-DO3A) ([HPTS]=100 nM, [Gd(HP-DO3A)]=0 - 2 mM, pH=6.5, λ_{exc}=455 nm, 0.15 M NaCl, 25°C)

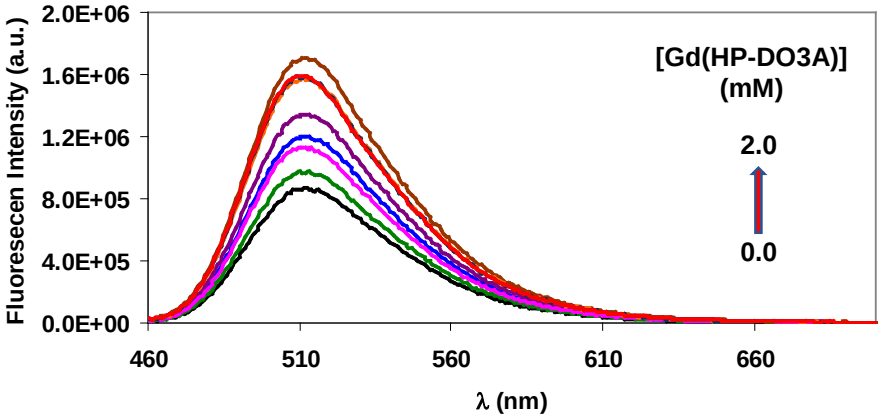

Figure S6. Emission spectra of HPTS in the presence and absence of Gd(HP-DO3A) ([HPTS]=100 nM, [Gd(HP-DO3A)]=0 - 2 mM, pH=7.0, λ_{exc}=455 nm, 0.15 M NaCl, 25°C)

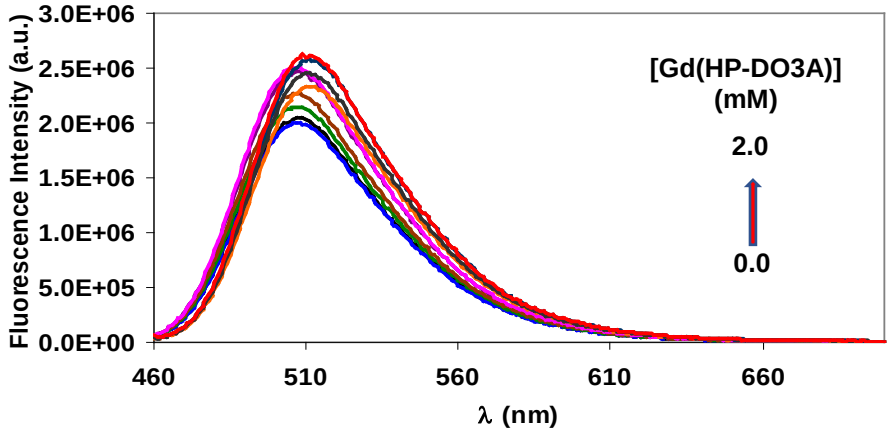

Figure S7. Emission spectra of HPTS in the presence and absence of Gd(HP-DO3A) ([HPTS]=100 nM, [Gd(HP-DO3A)]=0 - 2 mM, pH=8.0, λ_{exc}=455 nm, 0.15 M NaCl, 25°C)

The emission spectra of HPTS as a function of pH in the absence of Gd(HP-DO3A) have also been recorded with λ_{exc} = 405 and 455 nm and a slitwidth of 3 nm in the wavelength range 460 – 700 nm ([HPTS]=100 nM, 0.15 M NaCl). Emission spectra of HPTS are shown in Figures S8 and S9.

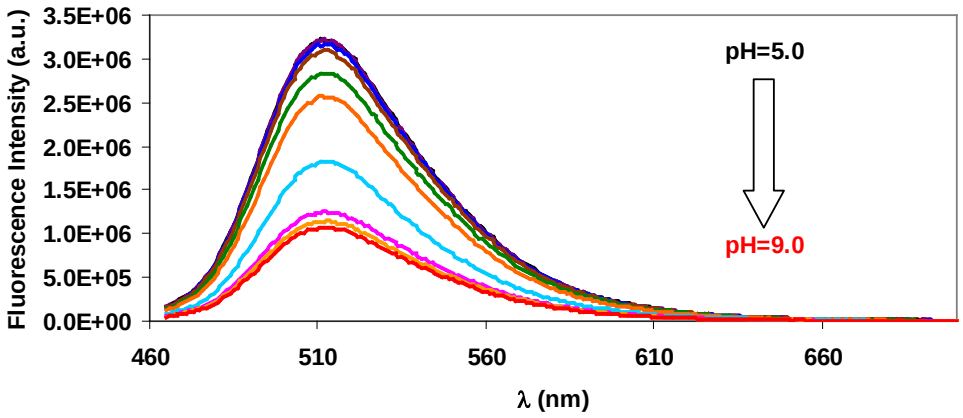

Figure S8. Emission spectra of HPTS as a function of pH ([HPTS]=100 nM, λ_{exc}=405 nm, 0.15 M NaCl, 25°C)

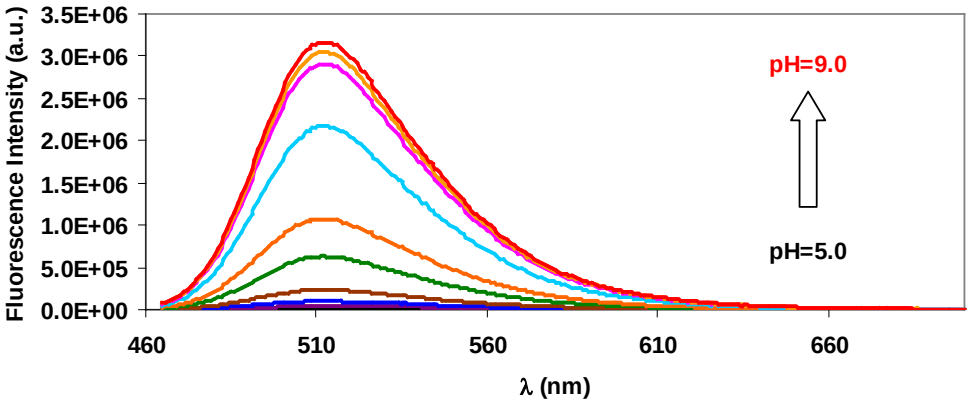

Figure S9. Emission spectra of HPTS as a function of pH ([HPTS]=100 nM, λ_{exc}=455 nm, 0.15 M NaCl, 25°C)

In order to confirm the direct proportion between the fluorescence intensity values and [HPTS], the emission spectra of 30, 60 and 100 nM HPTS solution have been recorded with λ_{exc} = 405 nm and 455 nm at pH=7.0 in 0.15 M NaCl (Figures S10 and S11). The fluorescence intensity values of HPTS with λ_{exc} = 405 nm and 455 nm at 511 nm increase monotonously with the increase of [HPTS], which clearly indicates the negligibility of the inner-filter effect [2]

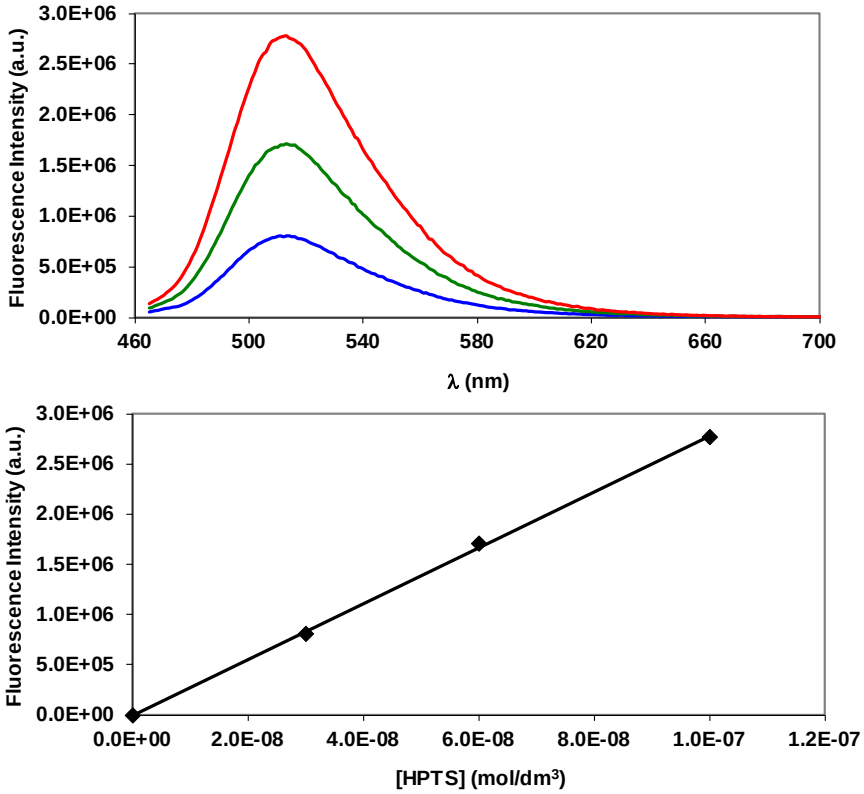

Figure S10. Emission spectra and fluorescence intensity of HPTS at 511 nm ([HPTS]=**30**, **60** and **100** nM, λ_{exc}=405 nm, 0.15 M NaCl, 25°C)

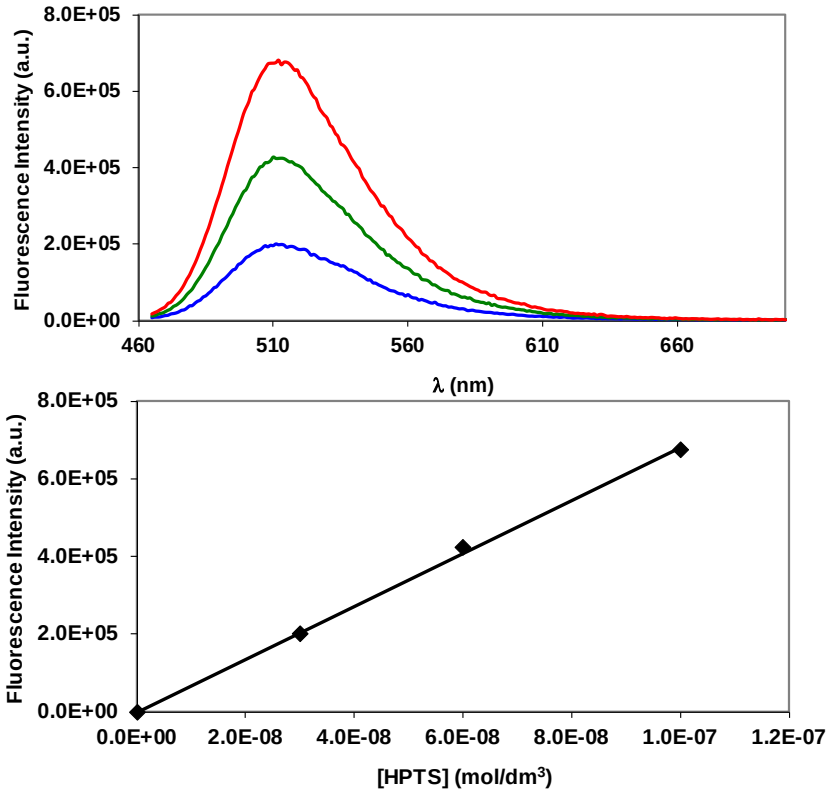

Figure S11. Emission spectra and fluorescence intensity of HPTS at 511 nm ([HPTS]=**30**, **60** and **100** nM, λ_{exc}=455 nm, 0.15 M NaCl, 25°C

As it is shown in Figures S2 – S4, the fluorescence intensity values of HPTS – Gd(HP-DO3A) systems with λ_{exc} = 405 nm decrease with the increase of [Gd(HP-DO3A)] at pH=6.5, 7.0 and 8.0 in the wavelength range 460 – 650 nm. However, the emission spectra of HPTS – Gd(HP-DO3A) systems with λ_{exc} = 455 nm reveal that the fluorescence intensity values increase with the increase of [Gd(HP-DO3A)] at pH=6.5, 7.0 and 8.0 in the wavelength range 460 – 650 nm (Figures S5 – S7). Moreover, the fluorescence intensity of HPTS with λ_{exc} = 405 and 455 nm decreases and increase with the increase of pH, respectively (Figures S8 and S9). The fluorescence intensity values of the HPTS as a function of pH and the HPTS – Gd(HP-DO3A) systems as a function of [Gd(HP-DO3A)] with λ_{exc} = 405 and 455 nm at 511 nm are shown in Figures S12 - S14.

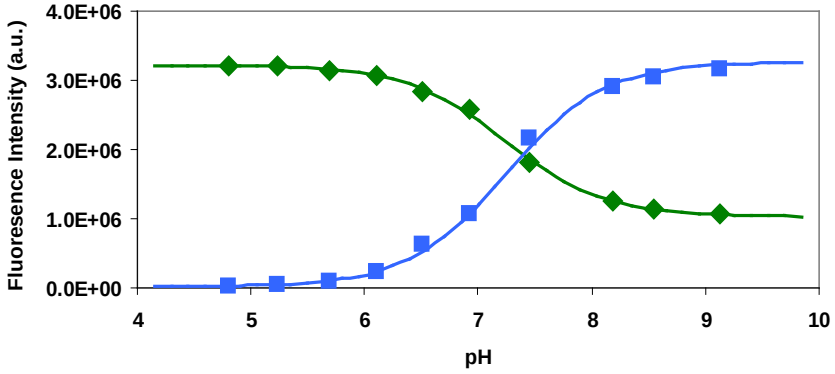

Figure S12. Fluorescence intensity of HPTS as a function of pH. The solid lines and the symbols represent the experimental and the calculated fluorescence intensity values, respectively. ([HPTS]=100 nM, λ_{exc}=405 nm (◆), λ_{exc}=455 nm (■), λ_{em}=511 nm, 0.15 M NaCl, 25°C)

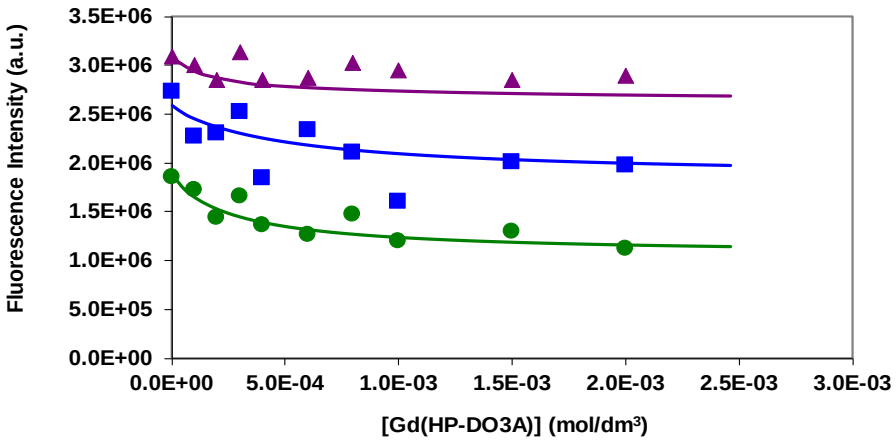

Figure S13. Fluorescence intensity of HPTS – Gd(HP-DO3A) systems at pH=**6.5**, **7.0** and **8.0**. The solid lines and the symbols represent the experimental and the calculated fluorescence intensity values, respectively. ([HPTS]=100 nM, λ_{exc}=405 nm, λ_{em}=511 nm, 0.15 M NaCl, 25°C).

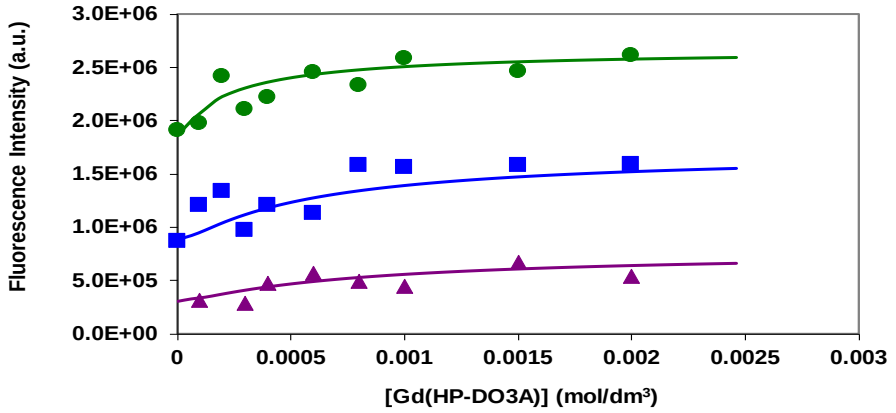

Figure S14. Fluorescence intensity of HPTS – Gd(HP-DO3A) systems at pH=**6.5**, **7.0** and **8.0**. The solid lines and the symbols represent the experimental and the calculated fluorescence intensity values, respectively. ([HPTS]=100 nM, λ_{exc}=455 nm, λ_{em}=511 nm, 0.15 M NaCl, 25°C)

The florescence intensity values of HPTS (Figure S12) and HPTS – Gd(HP-DO3A) systems (Figures S13 and S14) can be described by the protonation/deprotonation of HPTS (Eq. (S1)) and by formation of the GdL – T (Eq. (S3)), 2GdL – T (Eq. (S4)), GdL – HT (Eq. (S5)) and 2GdL – HT (Eq. (S6)) adducts with protonated (HT) and deprotonated (T) forms of HPTS molecule.

$$T + GdL \rightleftharpoons GdL\text{-}T \qquad (S3)$$

$$K_{GdL-T} = \frac{[GdL-T]}{[GdL][T]}$$

$$T + 2GdL \rightleftharpoons 2GdL\text{-}T \qquad (S4)$$

$$\beta_{2GdL-T} = K_{GdL-T} \times K_{2GdL-T} \frac{[2GdL-T]}{[GdL]^2[T]}$$

$$HT + GdL \rightleftharpoons GdL\text{-}HT \quad (S5)$$

$$\beta_{GdL-HT} = \frac{[GdL-HT]}{[GdL][HT]} = K_{GdL-HT} \times K^H = \frac{[GdL-HT]}{[GdL][H^+][T]}$$

$$HT + 2GdL \rightleftharpoons 2GdL\text{-}HT \quad (S6)$$

$$\beta_{2GdL-HT} = \frac{[2GdL-HT]}{[GdL]^2[HT]} = K_{GdL-HT} \times K_{2GdL-HT} \times K^H = \frac{[2GdL-HT]}{[GdL]^2[H^+][T]}$$

Figures S2 – S4 and S8 reveal that all HPTS containing species (T, HT, GdL–T, 2GdL – T, GdL – HT and 2GdL – HT) have an emission with λ_{exc}=405 nm at 511 nm. The florescence intensity values of HPTS and Gd(HP-DO3A) – HPTS systems in Figures S12 and S13 with λ_{exc}=405 nm at 511 nm can be expressed by Eq. (S7).

$$I = I_T + I_{HT} + I_{GdL-T} + I_{2GdL-T} + I_{GdL-HT} + I_{2GdL-HT} = k_T[T]_{free} + k_{HT}[HT]_{free} + k_{GdL-T}[GdL-T] + k_{2GdL-T}[2GdL-T] + k_{GdL-HT}[GdL-HT] + k_{2GdL-T}[2GdL-HT] \quad (S7)$$

where k_T, k_{HT} $k_{GdL\text{-}T}$, $k_{2GdL\text{-}T}$, $k_{GdL\text{-}HT}$, $k_{2GdL\text{-}HT}$ are the proportionality constants between I_T, I_{HT} $I_{GdL\text{-}T}$, $I_{2GdL\text{-}T}$, $I_{GdL\text{-}HT}$ and $I_{2GdL\text{-}HT}$ and $[T]_{free}$, $[HT]_{free}$, [GdL-T], [2GdL-T], [GdL-HT] and [2GdL-HT] with λ_{exc}=405 nm at 511 nm. By taking into account the total concentration of HPTS ($[T]_{tot}=[T]_{free}+[HT]_{free}+$[GdL-T]+[2GdL-T]+[GdL-HT]+[2GdL-HT]), Eqs. (S1), (S3) – (S6), $[T]_{free}$ can be expressed by Eq (S8).

$$[T]_{free} = \frac{[T]_{tot}}{1+K^H[H^+]+K_{GdL-T}[GdL]+\beta_{2GdL-T}[GdL]^2+K_{GdL-HT}K^H[H^+][GdL]+\beta_{2GdL-HT}[H^+][GdL]^2} = X \quad (S8)$$

By taking into account $[T]_{free}$ (Eq. (S8)) and Eq. (S7), the florescence intensity values of HPTS and Gd(HP-DO3A) – HPTS systems with λ_{exc}=405 nm at 511 nm can be expressed by Eq. (S9).

$$I = X \times (k_T + k_{HT}K^H[H^+] + k_{GdL-T}K_{GdL-T}[GdL] + k_{2GdL-T}\beta_{2GdL-T}[GdL]^2 + k_{GdL-HT}K_{GdL-HT}[H^+][GdL] + k_{2GdL-HT}\beta_{2GdL-HT}[H^+][GdL]^2) \quad (S9)$$

On the other hand, Figures S5 – S7 and S9 indicates that the deprotonated HPTS containing species (T, GdL–T, 2GdL – T,) have an emission only with λ_{exc}=455 nm at 511 nm. The florescence intensity values of HPTS and Gd(HP-DO3A) – HPTS systems in Figures S14 and S16 with λ_{exc}=455 nm at 511 nm can be expressed by Eq. (S10).

$$\boldsymbol{I = I_T + I_{GdL-T} + I_{2GdL-T} = k_T[T]_{free} + k_{GdL-T}[GdL-T] + k_{2GdL-T}[2GdL-T]} \quad (S10)$$

where k_T, $k_{GdL\text{-}T}$ and $k_{2GdL\text{-}T}$ are the proportionality constants between I_T, $I_{GdL\text{-}T}$ and $I_{2GdL\text{-}T}$ and $[T]_{free}$, [GdL-T] and [2GdL-T] with λ_{exc}=455 nm at 511 nm. By taking into account the total concentration of HPTS ($[T]_{tot}=[T]_{free}+[HT]_{free}+$[GdL-T]+[2GdL-T]+[GdL-HT]+[2GdL-HT]),

Eqs. (S1), (S3) – (S6), (S8) and (S10), the florescence intensity values of HPTS and Gd(HP-DO3A) – HPTS systems with λ_{exc}=455 nm at 511 nm can be expressed by Eq. (S11).

$$\boldsymbol{I = X \times (k_T + k_{GdL-T} K_{GdL-T}[GdL] + k_{2GdL-T} \beta_{2GdL-T}[GdL]^2)} \qquad \textit{(S11)}$$

The florescence intensity values of HPTS and Gd(HP-DO3A) – HPTS systems with λ_{exc}=405 and 455 nm at 511 nm as a function of pH and [Gd(HP-DO3A)] (Figures S12 – S14) were simultaneously fitted to Eqs. (S9) and (S11) in order to calculate the equilibrium constant characterizing the protonation (K^H) of HPTS and the formation of the GdL – T, 2GdL – T, GdL – HT and 2GdL – HT adducts and the proportionality constants (k_T, k_{HT} k_{GdL-T}, k_{2GdL-T}, k_{GdL-HT}, $k_{2GdL-HT)}$) for λ_{exc}=405 and 455 nm excitation with 511 nm emission. Equilibrium and proportionality constants characterizing the Gd(HP-DO3A) – HPTS systems are shown in Table S1.

Table S1. Stability constants of Gd(HP-DO3A) - HPTS adducts and the protonation constant of HPTS (0.15 M NaCl, 25°C)

Species	**log*K***
HHPTS (HT)	7.10 (1) (logK^H)
Gd(HP-DO3A) – HPTS (GdL-T)	4.5 (1)
2Gd(HP-DO3A) – HPTS (2GdL – T)	3.5 (1)
Gd(HP-DO3A) – HHPTS (GdL-HT)	4.3 (1)
2Gd(HP-DO3A) – HHPTS (2GdL-HT)	3.0 (2)

HPTS: logK^H= 7.29 ($[PO_4]_{tot}$=0.066 M, 22°C), Ref.[3]; λ_{exc}=405 nm: $k_T = 1.8\times10^{13}$ a.u./M; $k_{HT} = 3.9\times10^{13}$ a.u./M; $k_{GdL-T} = 1.5\times10^{13}$ a.u./M; $k_{2GdL-T}= 8.8\times10^{12}$ a.u./M; $k_{GdL-HT} = 3.1\times10^{13}$ a.u./M; $k_{2GdL-HT}= 3.3\times10^{13}$ a.u./M; λ_{exc}=455 nm: $k_T = 2.7\times10^{13}$ a.u./M; $k_{GdL-T} = 2.8\times10^{13}$ a.u./M; $k_{2GdL-T}= 2.9\times10^{13}$ a.u./M

By taking into account the protonation constant of the HPTS, the formation constant of the GdL-T, 2Gd-T, GdL-HT and 2GdL-HT adducts (Table S1), the species distribution of the Gd(HP-DO3A) - HPTS system as a function of [Gd(HP-DO3A)] has been calculated at pH=4.0 and 9.0 (Figure S15).

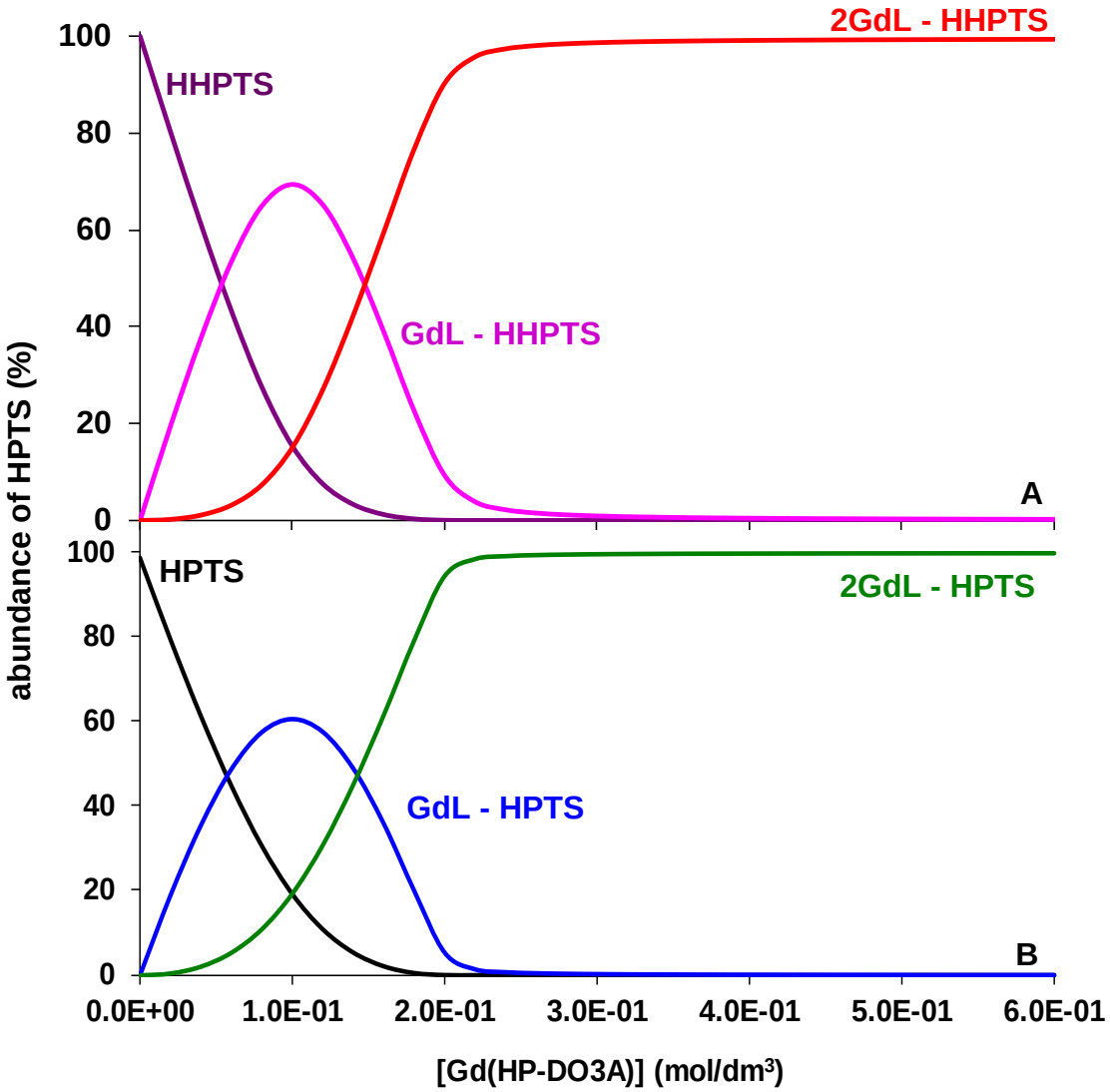

Figure S15. Species distribution of the Gd(HP-DO3A) - HPTS system at pH=4.0 (**A)** and 9.0 (**B)** ([HPTS]=0.1 M, 0.15 M NaCl, 25°C).

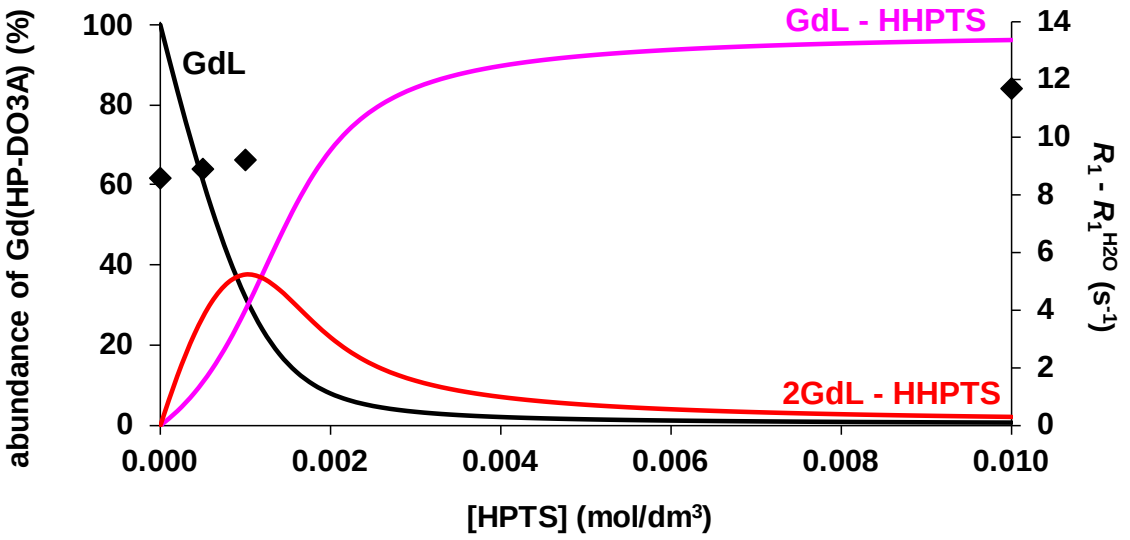

Figure S16. Species distribution and the relaxation rate ($R_1 - R_1^{H2O}$, ◆) of the Gd(HP-DO3A) - HPTS system as a function of [HPTS] at pH=5.0 ([Gd(HP-DO3A)]=1.97 mM, 21.5 MHz, 0.15 M NaCl, 25°C).

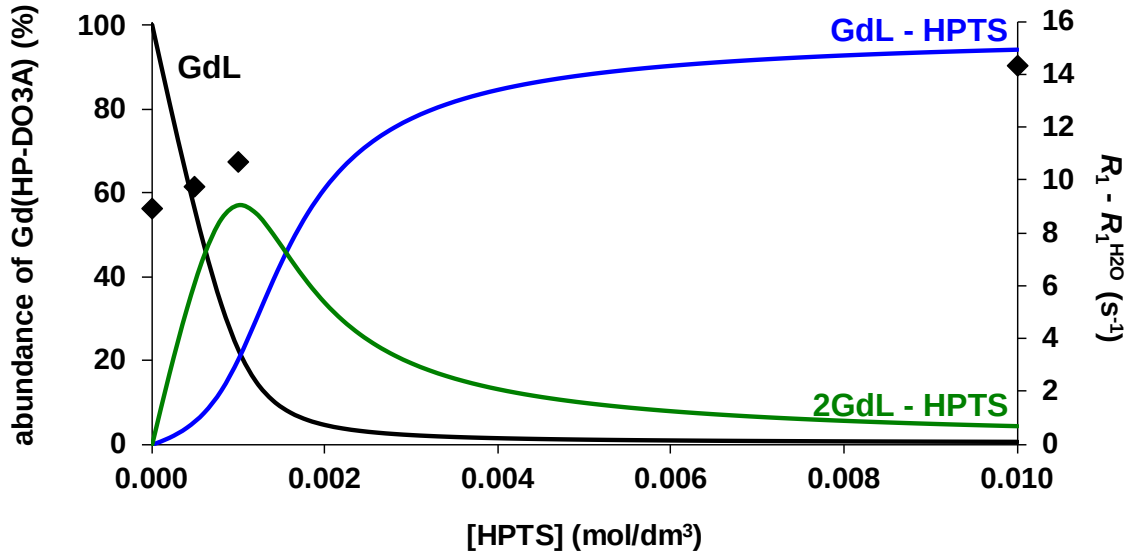

Figure S17. Species distribution and the relaxation rate ($R_1 - R_1^{H2O}$, ◆) of the Gd(HP-DO3A) - HPTS system as a function of [HPTS] at pH=9.0 ([Gd(HP-DO3A)]=2.0 mM, 21.5 MHz, 0.15 M NaCl, 25°C).

II. X-ray diffraction studies of the Gd(HP-DO3A) – HPTS adduct

II.1 Experimental

The structural properties of the Gd(HP-DO3A) – HPTS adducts has been examined with the single crystal X-ray diffraction studies in solid state. Crystallographic and experimental details of the data collection and refinement of the structure of $\{Gd(HP\text{-}DO3A)]_4(Na_3HPTS)\} \times H_2O$ and $\{(C(NH_2)_3)_3[Gd(HP\text{-}DO3A)]_8(Na_3HPTS)_3\} \times H_2O$ are reported in Tables S2-S6. Deposition Numbers 2149557-2149558 for $\{Gd(HP\text{-}DO3A)]_4(Na_3HPTS)\} \times H_2O$ (pH=4.0) and $\{(C(NH_2)_3)_3[Gd(HP\text{-}DO3A)]_8(Na_3HPTS)_3\} \times H_2O$ (pH=9.0) contain the supplementary crystallographic data, which are provided free of charge by the joint Cambridge Crystallographic Data Centre and Fachinformationszentrum Karlsruhe Access Structures service. All esds (except the esd in the dihedral angle between two l.s. planes) are estimated using the full covariance matrix. The cell esds are taken into account individually in the estimation of esds in distances, angles and torsion angles; correlations between esds in cell parameters are only used when they are defined by crystal symmetry. An approximate (isotropic) treatment of cell esds is used for estimating esds involving l.s. planes.

Table S2. Experimental details of X-ray structure determination.

	{Gd(HP-DO3A)]$_4$(Na$_3$HPTS)}×H$_2$O	{(C(NH$_2$)$_3$)$_3$[Gd(HP-DO3A)]$_8$(Na$_3$HPTS)$_3$}×H$_2$O
Crystal data		
Chemical formula	$C_{84}H_{180}Gd_4N_{16}Na_3O_{70.50}S_3$	$C_{185}H_{333}Gd_8N_{35}Na_{11}O_{128}S_9$
M_r	3336.58	6895.27
Crystal system, space group	Triclinic, *P*1	Monoclinic, $P2_1/n$
Temperature (K)	150	150
a, *b*, *c* (Å)	11.0385 (7), 18.5193 (13), 19.2191 (14)	10.9363 (4), 49.0025 (18), 30.2223 (13)
α, β, γ (°)	62.497 (3), 79.100 (3), 85.447 (3)	90, 90.01 (1), 90
V (Å^3)	3421.8 (4)	16196.3 (11)
Z	1	2
Radiation type	Mo *K*α	
μ (mm^{-1})	2.07	1.77
Crystal size (mm)	0.44 × 0.23 × 0.21	0.21 × 0.10 × 0.06
Data collection		
Diffractometer	Bruker D8 VENTURE	
Absorption correction	Multi-scan *SADABS2016*/2 - Bruker AXS area detector scaling and absorption correction	
T_{min}, T_{max}	0.46, 0.67	0.71, 0.90
No. of measured, independent and observed [$I > 2\sigma(I)$] reflections	131387, 31973, 24975	151344, 31906, 25658
R_{int}	0.078	0.054
$(\sin\theta/\lambda)_{max}$ (Å^{-1})	0.668	0.618
Refinement		
$R[F^2 > 2\sigma(F^2)]$, $wR(F^2)$, *S*	0.059, 0.123, 1.04	0.084, 0.259, 1.12
No. of reflections	31973	31906
No. of parameters	1586	1834
No. of restraints	326	2116
H-atom treatment	H atoms treated by a mixture of independent and constrained refinement	
	$w = 1/[\sigma^2(F_o^2) + (0.0427P)^2 + 21.2367P]$ where $P = (F_o^2 + 2F_c^2)/3$	$w = 1/[\sigma^2(F_o^2) + (0.127P)^2 + 158.0355P]$ where $P = (F_o^2 + 2F_c^2)/3$
$(\Delta/\sigma)_{max}$	0.306	0.003
$\Delta\rangle_{max}$, $\Delta\rangle_{min}$ (e Å^{-3})	2.06, -1.29	3.14, -1.38
Absolute structure	Refined as an inversion twin.	–
Absolute structure parameter	0.494 (18)	–

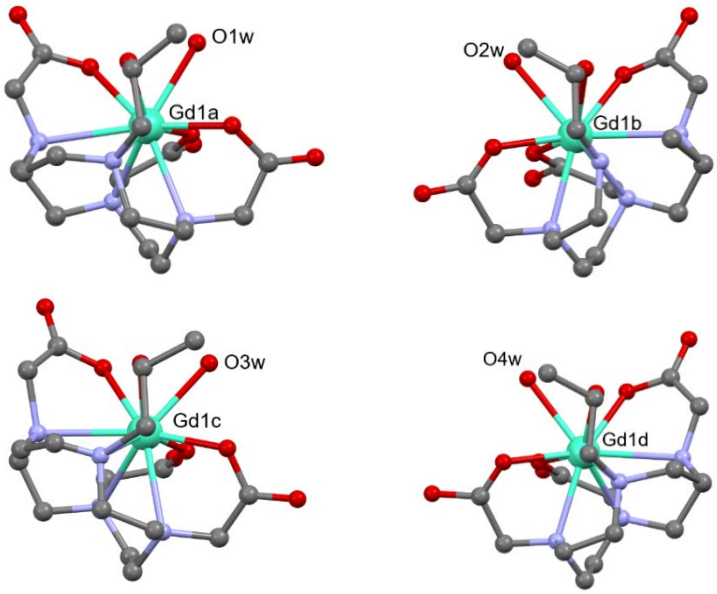

Figure S18. View of the four Gd(HP-DO3A) complexes present in the single crystal of {[Gd(HP-DO3A)]$_4$(Na_3HPTS)} (pH=4.0). Hydrogen atoms are omitted for simplicity. Color code: Gd (green), O (red), N (blue), and C (grey).

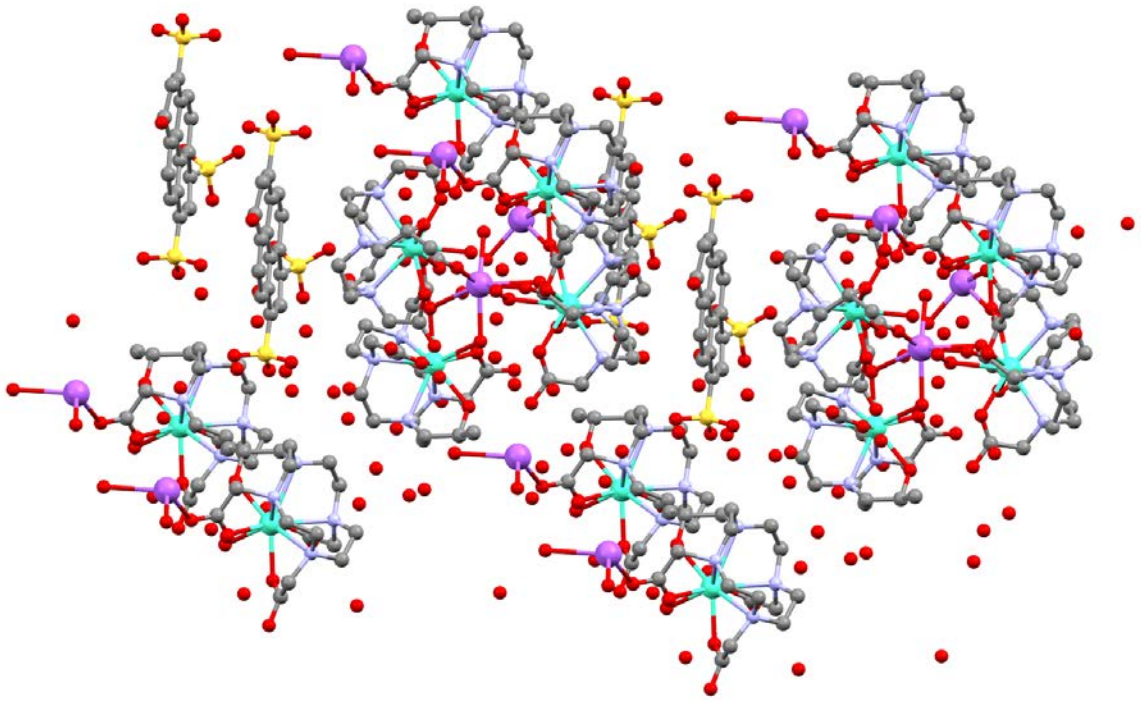

Figure S19. Packing diagram of {Gd(HP-DO3A)]$_4$(Na_3HPTS)}. Hydrogen atoms are omitted for simplicity.

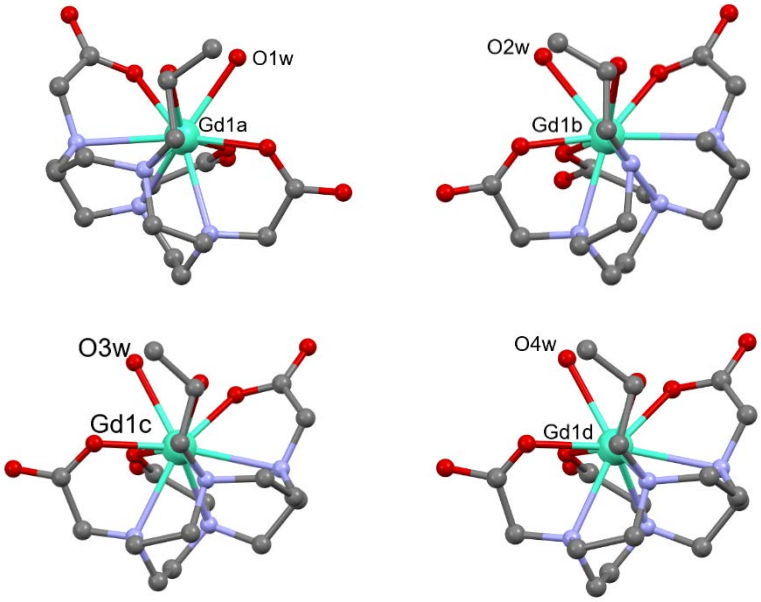

Figure S20. View of the four Gd(HP-DO3A) complexes present in the single crystal of $\{(C(NH_2)_3)_3[Gd(HP\text{-}DO3A)]_8(Na_3HPTS)_3\}$ (pH=9.0). Hydrogen atoms are omitted for simplicity. Color code: Gd (green), O (red), N (blue), and C (grey).

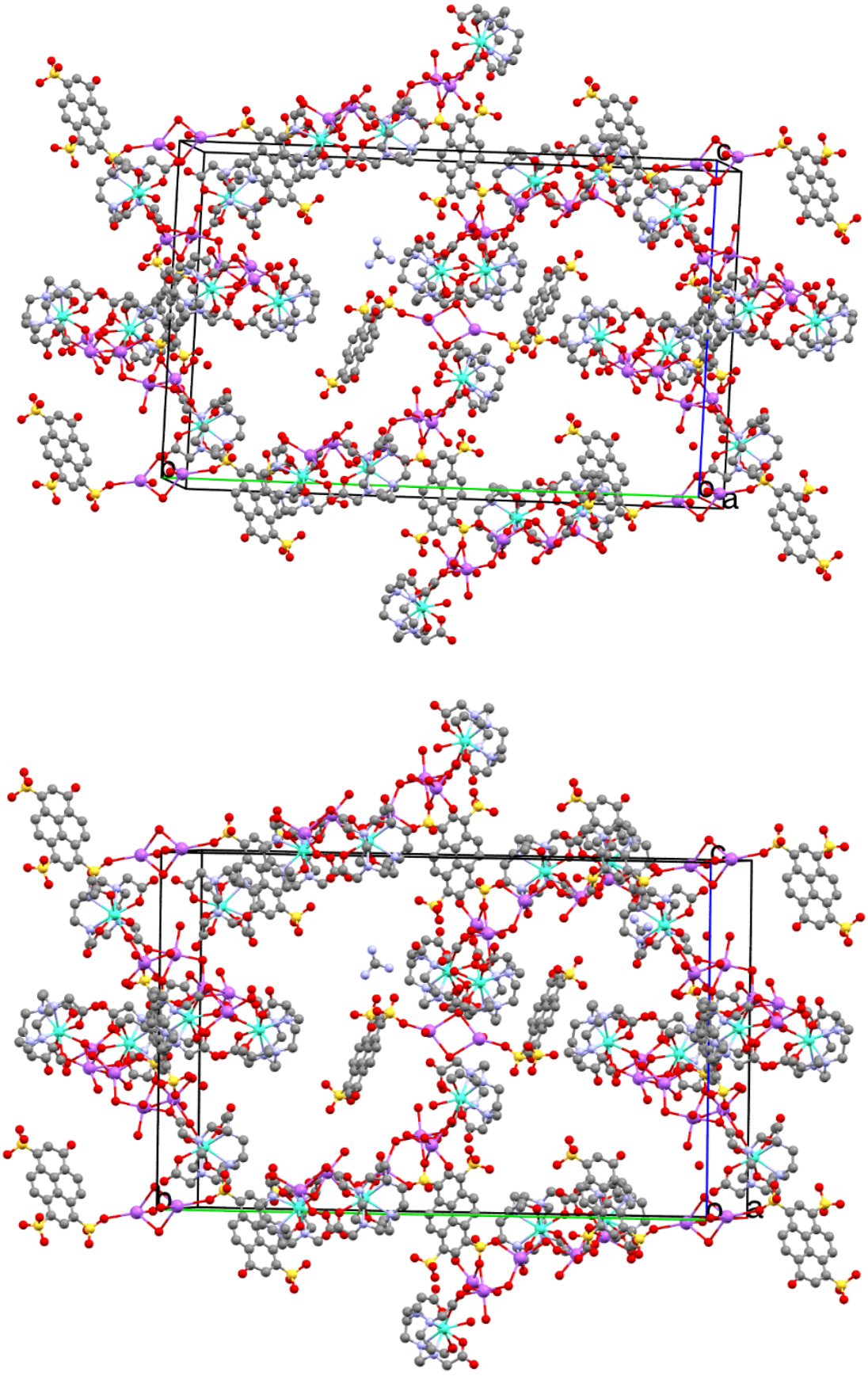

Figure S21. Packing diagram of $\{(C(NH_2)_3)_3[Gd(HP\text{-}DO3A)]_8(Na_3HPTS)_3\}$. Hydrogen atoms are omitted for simplicity.

II.2 X-ray diffraction studies of solid state Gd(HPDO3A)-HPTS adducts at pH=4 and pH=9.0

The X-ray structure of [Gd(HP-DO3A) complexes in Gd(HP-DO3A)-HPTS adduct is similar to that of [Gd(HP-DO3A)(H_2O)].[5] The crystallization of the racemic [Gd(HP-DO3A)(H_2O)] takes place by the formation of dimers with capped square antiprismatic (SAP) and capped twisted square antiprism (TSAP) diastereomers of equimolar R and S isomers.[4] The Gd(III)-ion is placed between the two nearly parallel planes formed by nitrogen atoms of the macrocycle and the oxygen atom of the pendant arms. The torsion angle between the two planes defined by the square of oxygen and nitrogen atoms are 38° and -28° for the SAP and TSAP stereoisomers of [Gd(HP-DO3A)(H_2O)], respectively. The distance of the Gd(III) ion from the planes formed by nitrogen and the oxygen atoms are 1.61 and 0.75 Å for the SAP and 1.68 and 0.78 Å for TSAP stereoisomers, respectively. The Gd – N and Gd – O distances in [Gd(HP-DO3A)(H_2O)] complex are in the range of 2.64 - 2.65 and 2.31 - 2.38 Å, respectively.

The X-ray diffraction studies of Gd(HP-DO3A)-HPTS adduct obtained at pH=4.0 and 9.0 reveal that donor atoms of the macrocycle in [Gd(HP-DO3A)(H_2O)] units encapsulate the central Gd(III)-ion which is placed between the four coplanar nitrogen atoms of the ring (N1, N4, N7 and N10) and the four coplanar oxygen atoms of three acetic and the 2-hydroxypropyl pendant arms (OH, O1, O4 and O71). The ninth apical coordination site of Gd(III)-ion is occupied by a water molecule to complete the SAP or TSAP geometry. Selected distances (Å) and angles (°) of the Gd(HP-DO3A)-HPTS adduct at pH=4.0 and 9.0 are shown in Tables S3 and S4. In Gd(HP-DO3A)-HPTS adduct obtained at pH=4.0 the distances of the Gd(III)-ion from OH, O1, O4 and O71 and N1 - N4 - N7 - N10 planes are in the range of 0.789 – 0.845 Å and 1.605 – 1.766 Å, respectively. The torsion angle between the two square planes defined by the oxygen and nitrogen atoms is 22.2, -29.4, 16.5 and -26.5° for Gd1A, Gd1B, Gd1C and Gd1D isomers, respectively. The distances of Gd(III)-ion with the coordinated N and O donor atoms of HP-DO3A are in the ranges of 2.56 – 2.72 Å and 2.27–2.41 Å, respectively. In Gd(HP-DO3A)-HPTS adduct obtained at pH=9.0 the distance of the Gd(III) ion from OH, O1, O4 and O7 and N1 - N4 - N7 - N10 planes is in the range of 0.804 – 0.846 Å and 1.647 – 1.672 Å, respectively. The torsion angle between the two square planes defined by the oxygen and nitrogen atoms is 26.2, -25.1, -22.9 and -22.3° for Gd1a, Gd1b, Gd1c and Gd1d isomers, respectively. Distances of Gd(III) with the coordinated N and O donor atoms of HP-DO3A are in the ranges of 2.61 – 2.70 Å and 2.34–2.40 Å, respectively.

Table S3. Selected distances (Å) and angles (°) of the Gd(HP-DO3A)-HPTS adduct at pH=4.0. (Standard deviations are shown in parentheses).

	Gd1A	Gd1B	Gd1C	Gd1D
Gd - Ow	2.517(13)	2.550(13)	2.535(13)	2.528(14)
Gd - OH	2.398(13)	2.383(15)	2.393(14)	2.368(14)
Gd – O1	2.348(14)	2.412(14)	2.341(16)	2.399(14)
Gd – O4	2.300(15)	2.334(15)	2.385(15)	2.382(16)
Gd – O7	2.385(14)	2.338(14)	2.304(15)	2.366(13)
Gd – N1	2.659(17)	2.677(12)	2.719(12)	2.68(2)
Gd – N4	2.654(17)	2.594(11)	2.730(10)	2.677(14)
Gd – N7	2.704(19)	2.567(12)	2.727(10)	2.610(17)
Gd – N10	2.65(2)	2.608(12)	2.739(12)	2.70(2)
Conformation	Λ(λλλλ)	Δ(δδδδ)	Λ(λλλλ)	Δ(δδδδ)
Tor. angle (°) Isomers	22.2 SAP	-29.4 TSAP	16.5 SAP	-26.5 TSAP

Table S4. Selected distances (Å) and angles (°) of the Gd(HP-DO3A)-HPTS adduct at pH=9.0. (Standard deviations are shown in parentheses).

	Gd1a	Gd1b	Gd1c	Gd1d
Gd - Ow	2.487(7)	2.518(6)	2.556(7)	2.525(6)
Gd - OH	2.377(7)	2.390(7)	2.393(9)	2.393(6)
Gd – O1	2.360(7)	2.341(7)	2.387(7)	2.340(6)
Gd – O3	2.349(7)	2.355(7)	2.354(10)	2.365(7)
Gd – O5	2.381(7)	2.396(7)	2.356(8)	2.382(7)
Gd – N1	2.603(10)	2.646(9)	2.693(11)	2.619(8)
Gd – N4	2.678(8)	2.628(10)	2.662(10)	2.682(8)
Gd – N7	2.683(9)	2.680(9)	2.643(10)	2.677(8)
Gd – N10	2.654(9)	2.649(9)	2.622(12)	2.649(8)
Conformation	Λ(λλλλ)	Δ(δδδδ)	Δ(δδδδ)	Δ(δδδδ)
Tor. angle (°) Isomers	26.2 SAP	-25.1 TSAP	-22.9 TSAP	-22.3 TSAP

III. In vitro optical and ex vivo MRI and optical imaging

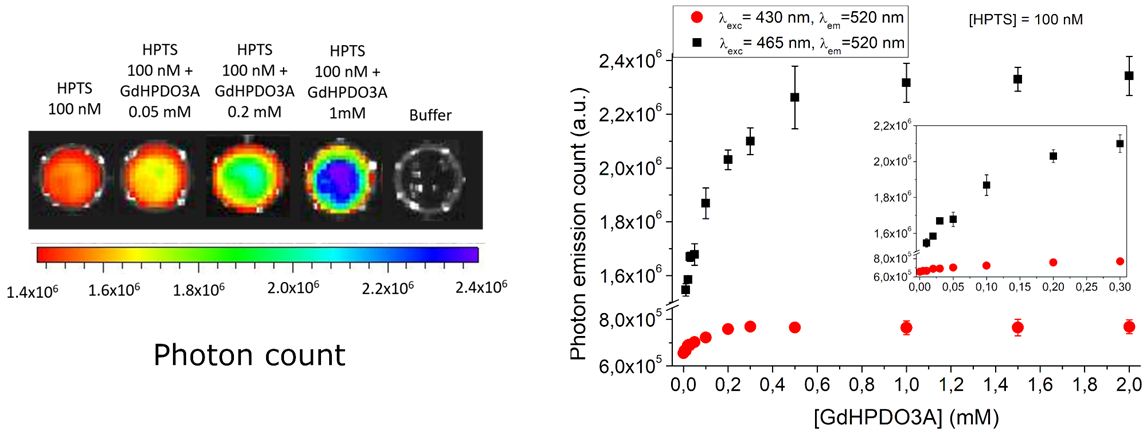

Figure S22. Fluorescence experiments, the *in vitro* phantom definitively showed that the co-presence of Gd(HP-DO3A) and HPTS can be detected by optical imaging.

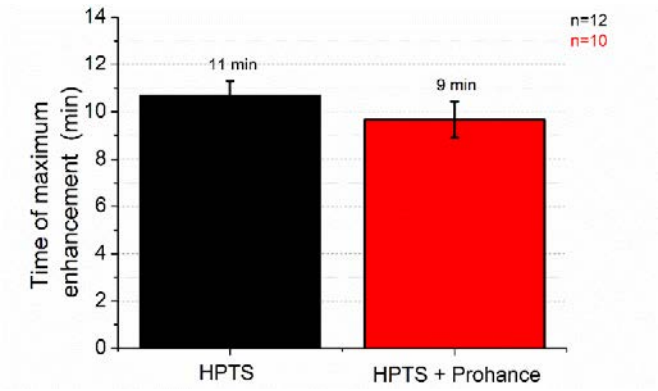

Figure S23. Time of maximum signal enhancement for HPTS (black) or Gd(HP-DO3A) - HPTS adduct (red).

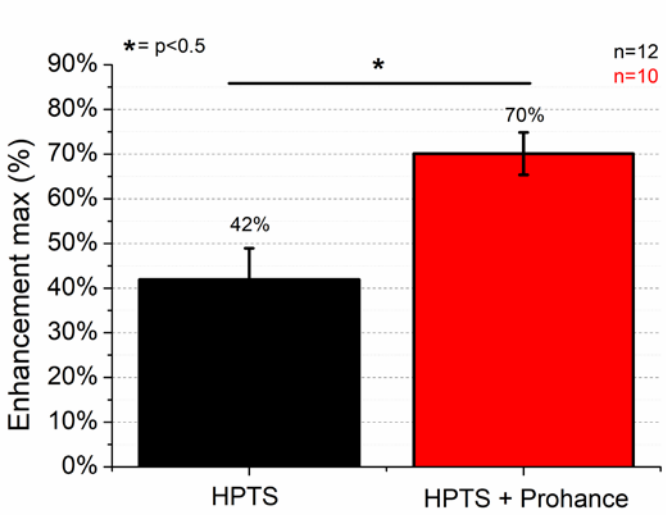

Figure S24. Maximum signal enhancement reached after injection of HPTS (*black*) or Gd(HP-DO3A)- HPTS adduct (*red*).

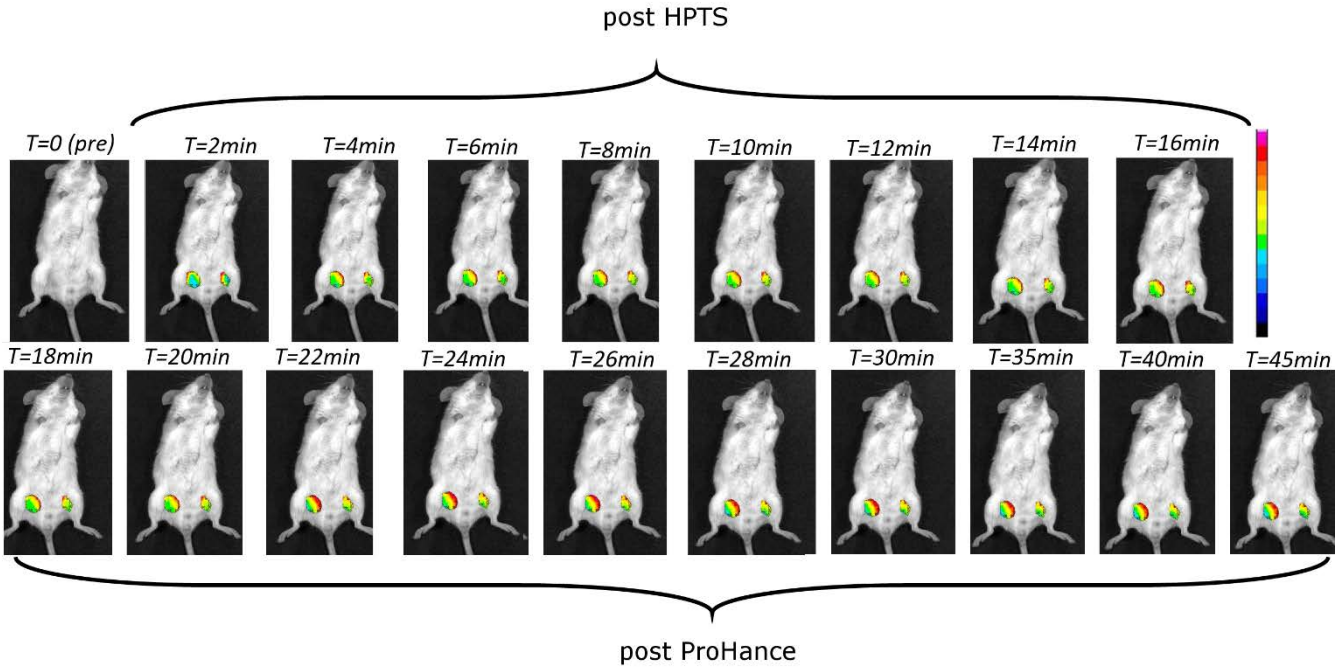

Figure S25. FLI images showing the fluorescence signal *pre* HPTS, *post* HPTS and *post* Gd(HP-DO3A) at variable time points.

Since the *in vivo* fluorescence enhancement is directly proportional to the concentration of HPTS containing species and the *wash-in* and *wash-out* processes can be regarded as a parallel pseudo-first-order processes, rate constants (k_α, k_β) and half-life ($t_{1/2}$ α/β =ln2/ $k_{\alpha/\beta}$) values characterizing the *wash-in* and *wash-out* of HPTS and HPTS – Gd(HPDO3A) adducts in the tumor region were calculated by fitting of the enhancement vs. time data pairs (Figure 7) to Eqs. (S12) and (S13), respectively.

$$E_t = (E_0 - E_f)e^{-k_\alpha^{HPTS}t} + (E_f - E_p)e^{-k_\beta^{HPTS}t} + E_p \qquad (S12)$$

$$E_t = (E_0 - E_f)e^{-k_\alpha^{Add}t} + (E_f - E_q)e^{-k_\beta^{Add}t} + (E_q - E_p)e^{-k_\beta^{HPTS}t} + E_p \qquad (S13)$$

where k_α^{HPTS}, k_β^{HPTS}, k_α^{Add} and k_β^{Add} are the pseudo-first-order rate constants characterizing the *wash-in* and *wash-out* of HPTS and HPTS – Gd(HPDO3A) adduct in the tumor region. E_t, E_0, E_f, E_q and E_p are the enhancement values at time t, at the beginning, at the end of the first and second part and at the end of the excretion, respectively. In the fitting procedure, values of E_0 and E_p were fixed to zero.

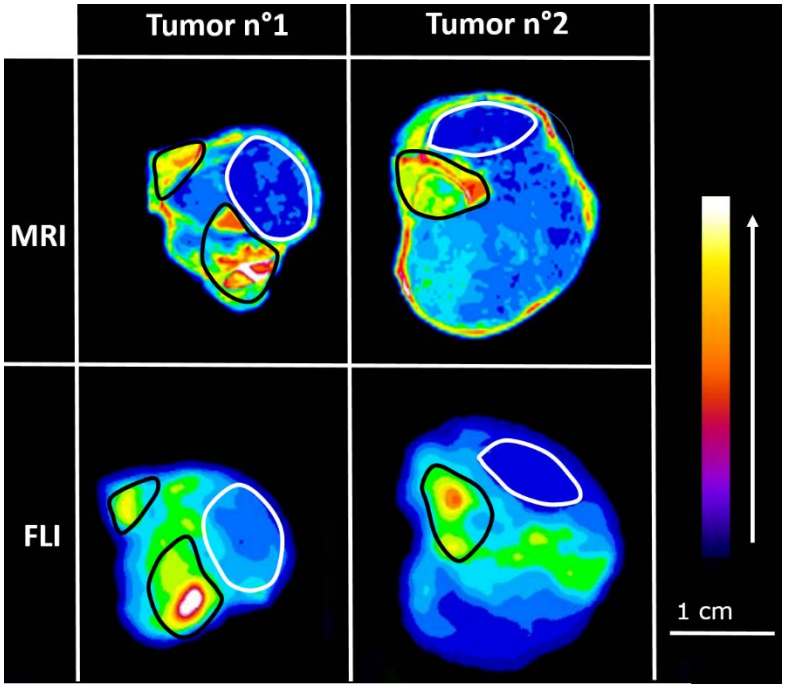

Figure S26. *Ex vivo* MRI and optical imaging analysis of excised tumors. White ROIs indicate regions of low signal intensity; Black ROIs indicate regions of high signal intensity.

IV. References

1 M. T. Beck and I. Nagypal, *Chemistry of Complex Equilibria*, Horwood, 1990.

2 M. van de Weert and L. Stella, Fluorescence quenching and ligand binding: A critical discussion of a popular methodology, *J. Mol. Struct.*, 2011, **998**, 144–150.

3 O. S. Wolfbeis, E. Fürlinger, H. Kroneis and H. Marsoner, Fluorimetric Analysis, *Z. Anal. Chem.*, 1983, **314**, 119–124.

4 K. Kumar, C. A. Chang, L. C. Francesconi, D. D. Dischino, M. F. Malley, J. Z. Gougoutas and M. F. Tweedle, Synthesis, Stability, and Structure of Gadolinium(III) and Yttrium(III) Macrocyclic Poly(amino carboxylates), *Inorg. Chem.*, 1994, **33**, 3567–3575.